

Chapter 4

MODIFICATIONS ON THE (PEXEP) PINCER PLATFORM: THERMODYNAMICS AND KINETICS OF CO₂ REDUCTION AND HYDROGEN EVOLUTION

With contributions from Sean Najmi, Yufeng Huang, David Shaffer, Robert J. Nielsen,
Jenny Yang, and William A. Goddard III

Some material adapted from:

D.W. Shaffer, **S.I. Johnson**, J.W. Ziller, R.J. Nielsen, W.A. Goddard, A.L. Rheingold, J.Y. Yang; Reactivity of a Series of Isostructural Cobalt Pincer Complexes with CO₂, CO, and H⁺. *Inorganic Chemistry*. 2014. 53 (24) 13031

Introduction

In the previous chapter, we work towards the goal of using solar power to electrochemically reduce CO₂ (CO₂RR) to formate or higher order reduction products.¹⁻³ In this chapter, we continue that work through systematic modification to understand why so few catalysts are able to complete this reaction selectively, as competition by proton reduction leading to the hydrogen evolution reaction (HER) is often present.^{4,5} Two notable successful exceptions stand out: (POCOP)Ir ([C₆H₃-2,6-[OP(*t*Bu)₂]₂]IrH₂), as made by Meyer and Brookhart⁶⁻⁹ and the mechanism described in the previous chapter, and [Fe₄N(CO)₁₂]⁻, as made by Berben and coworkers¹⁰. Both catalysts are able to reduce CO₂ to formate in water without significant competition from HER. In the case of (POCOP)Ir, Faradaic efficiency of 93% is achieved, with the competing HER shown to occur at the electrode rather than the Ir catalyst.⁸ Berben sees 96% Faradaic efficiency in [Fe₄N(CO)₁₂]⁻ clusters.¹⁰ Despite the selectivity of the parent compound, substitution of the N atom for carbon in the tetrairon clusters exclusively produces H₂.¹¹ Our group recently studied the mechanism for CO₂RR by (POCOP)Ir via density functional theory (DFT) with the goal of understanding its impressive selectivity, showing that hydrogen production was limited by high kinetic barriers for protonation of the Ir dihydride.¹² In both Berben and our studies, hydricity, or the ability of a hydride donor to give up a hydride, was calculated, either experimentally or computationally. When compared to another hydricity, it can indicate the thermodynamic driving force for donation from a hydride donor to a hydride acceptor. The hydricity of a transition metal complex can be obtained through a variety of

methods, though most recent measurements involve use of a thermodynamic cycle.⁵ They are also often referenced to the reaction of a proton and a hydride to make H₂.¹³ These measurements are also often made at equilibrium, so little indication of a H⁻ transfer rate is made, though occasionally kinetic hydricities have been measured.¹⁴ Hydricities as a design principle have been used previously, both in catalyst design¹⁵⁻¹⁹ and in understanding the effect of experimental conditions.²⁰⁻²² In order to donate a hydride to CO₂ to make formate, the hydricity of the compound must be less than 24 kcal/mol, or the hydricity of the CO₂/HCOO⁻ couple. Theoretically, however, no lower bound to this range exists, except that too low a hydricity represents unnecessary energy input into the system. The hydricity of (POCOP)Ir in water was calculated to be 18.6 kcal/mol, (referenced to a $\Delta G_{\text{water}}(\text{H}^+ + \text{H}^- \rightarrow \text{H}_2) = 34.2$ kcal/mol¹³). Experimentally, the hydricities of the [Fe₄N(CO)₁₂]⁻ and [Fe₄C(CO)₁₂]²⁻ complexes were calculated to be 15.5 and <15 kcal/mol, respectively.¹¹ Since the carbon analog catalyst did evolve hydrogen, Berben and coworkers proposed a “formate window”. This window establishes a lower bound to the range of suitable hydricities by suggesting that in complexes with hydricities lower than 15 kcal/mol, selectivity for CO₂RR over HER would be lost¹¹ as driving force for HER would be too strong. Previous (POCOP)Ir work appears to support this, as a monohydride anion complex on the path of CO₂RR has a calculated hydricity of 5.4 kcal/mol and sees faster protonation than CO₂RR ($\Delta G_{\text{HER}}^\ddagger = 6.3$ kcal/mol vs $\Delta G_{\text{CO}_2\text{RR}}^\ddagger = 13.8$ kcal/mol), though hydrogen evolution is limited by isomerization to the Ir dihydride.¹² If indeed a hydricity range for kinetically preferred CO₂RR exists, this could become a powerful screening tool for both experiment and theory to predict selective CO₂RR catalysts.

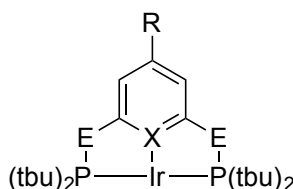


Figure 4.1: POCOP-Ir is substituted in the *para* position (R) with -NH₂, -OH, -Me, -H, and -CF₃, the arm groups (E) with -CH₂ and -O and the *ipso* position (X) with -C and -N to change the electronic structure of the catalyst.

In order to probe this possibility, the barriers for hydride transfer to CO₂ and protonation of the hydride in a series of modified tridentate pincer (*p*-R-C₅XH₃-2,6-[EP(*t*Bu)₂]₂) complexes have

been calculated. One strength of using pincers is that their highly modular nature enables them to be methodically altered. In particular, substitution in the *para* position on the phenyl ring can change the electronic structure in the metal center in an isolated manner without significantly changing the steric interactions at the reaction center.²³ Computational studies in both substituted pincers and other complexes have been previously used to investigate a variety of catalytic processes, including hydrogen evolution²⁴, hydrogenation²⁵, C-H activation^{26,27}, and water-splitting²⁸. Experimentally, substituted POCOP catalysts have been used to study silane dehydrocoupling²⁹ and dehydrogenation²⁶. The substituted R-POCOP pincer can be seen in Figure 4.1. Various R groups (R = -NH₂, -OH, -Me, -H, -CF₃) were chosen to represent a range of Hammett constants (σ_p between -0.66 and 0.54)³⁰ to probe both electron donating and withdrawing effects. These complexes will be used in particular for the hydricity studies. Calculated hydricities of these compounds can be seen in Table 4.1, where they span the range 21.1 to 15.2 kcal/mol. In addition to kinetic effects, electronic effects on acetonitrile (MeCN) coordination and intermediate energies will be investigated.

For understanding general effects, pincer ligands can also be modified in the *ipso* position (X in Figure 4.1), substituting the phenyl ring for other aromatic (or non-aromatic³¹) rings, as well as the arms (E). Prior work has investigated the use of both (POCOP)Co^{12,32} and for use in CO₂RR, while experimental work has investigated (PONOP)Ir for use in C-H bond cleavage.³³ Here, we will investigate (PENEP)Co (E = CH₂, O) catalysts, then compare to (PONOP)Ir.

While some of these systems have been made experimentally^{29,34,35}, it is important to note that these pincers are primarily toy systems.

Methods

All geometry optimizations, frequency and solvation calculations were carried out using the B3LYP functional³⁶ and with a 2- ζ basis set and the Los Alamos small core potential on iridium and 6-311G** basis set on organics.^{37,38} Single point electronic calculations were completed with the M06 functional.³⁹ The LACVP**++ basis set was used in iridium with augmented *f*-functions and diffuse functions.⁴⁰ All organic atoms used the 6-311G**++ basis set.⁴¹ Solvation in water was modeled using the Poisson-Boltzmann polarizable continuum model using a dielectric constant of 80.37 and probe radius of 1.40 Å. In order to calculate the free energy of acetonitrile

in water, the 1 atm ideal gas free energy of MeCN was computed using appropriate statistical mechanical methods and empirical free energies of vaporization (2.45 kcal/mol⁴²) was subtracted. Solvation of formate in water was taken from experiment.⁴³

In the case of (PENEP)Co catalysts, B3LYP-D3, the dispersion corrected functional was used.⁴⁴ Solvation for these complexes in acetonitrile via the Poisson Boltzmann polarizable continuum model used a dielectric constant of 37.5 and a probe radius of 2.19 Å. The free energy of 1 M acetonitrile was computed using the appropriate statistical mechanics formulae, and the empirical free energies of vaporization (1.27 kcal/mol, derived from the vapor pressure^{42,45}) was subtracted. The chemical potential of H⁺(1M) in MeCN was the ideal gas free energy ($H-TS = 5/2 kT - (298K)(26.04 \text{ e.u.})^{46} = -6.3 \text{ kcal/mol}$) minus the free energy of hydration ($\Delta G(1\text{atm}\rightarrow 1\text{M}) = 264.0 \text{ kcal/mol}^{47}$) plus the transfer free energy $\Delta G(1\text{M, aq}\rightarrow 1\text{M, MeCN}) = 5.7 \text{ kcal/mol}^{48}$]. The formally “Co⁰” solvent complexes are best described as high spin, cationic Co^I centers antiferromagnetically coupled to radical anionic pyridine ligands. The approximate projection scheme proposed by Yamaguchi⁴⁹ was applied (using the large basis, unsolvated wavefunctions) to correct electronic energies of the unrestricted doublets for spin-contamination from the higher-energy quartet state, S^2 values of the broken-symmetry doublets ranged from 1.50 to 1.65, leading to corrections of up to 3.2 kcal/mol. Wavefunctions for Co^{II} and Co^I states did not suffer spin contamination.

Free energies were calculated by the following equation:

$$G = E_{M06} + G_{solv} + E_{ZPE} + H_{vib} + H_{TR} - T(S_{vib} + S_{elec} + S_{TR})$$

In this equation, E_{M06} , G_{solv} , and E_{ZPE} are the single point electronic energy, free energy of solvation, and zero-point energy correction, respectively. H_{vib} and H_{TR} ($^{12}/_2 k_B T$) are the vibrational and translational/rotational enthalpies respectively, while S_{vib} , S_{elec} , and S_{TR} represent the vibrational, electronic, and translational/rotational entropies. Gas phase translational and rotational entropies were modified by corrections suggested by Wertz in order to be used in solvent.⁵⁰ Transition state calculations were validated by the presence of imaginary modes in analytical frequency calculations. All calculations were carried out in Jaguar.⁵¹

Hydricities were calculated using the free energy from the following equation:



where L is the modified pincer ligand. In order to calculate the free energy of the proton in solution for hydricity calculations, we are using the value established by Tissandier and coworkers.⁴⁷ In the previous chapter¹², we have referenced hydricities to the H₂/H⁺ couple, but for the sake of comparison to experimental systems we are referencing hydricities to the free energy of the formation of hydrogen from a proton and a hydride (34.2 kcal/mol in water), in accordance with recommendations set forth by Connelly et al.¹³ These are the same values used by Berben and coworkers.¹¹

Results and Discussion

Effect of Modification on Pathways and Hydricity

Low energy pathways for the CO₂RR and protonation of the ground state (H-POCOP)Ir complex have been previously modeled¹² and will serve as the template for mechanistic steps in the modified complexes. Free energy surfaces for three representative compounds (X= NH₂, H, and CF₃) can be seen in Figure 4.2, with all pincer complexes represented in Appendix B in the Supporting Information. The complexes whose pathways are shown in Figure 4.2 were chosen because they are the most electron donating/withdrawing groups according to Hammett constant. The pathway for CO₂RR is shown moving from **Mol 1** (in the center) to the right. MeCN first coordinates to form **Mol 1b**, after which the hydride can be abstracted in **TS 1**. The subsequent formate complex, bound through the hydride, is shown in **Mol 2**. In water, the formate ion can be solvated and thus dissociates to form **Mol 3**. Finally, a second MeCN molecule can coordinate to form the octahedral complex **Mol 4**, which can then undergo a two electron reduction and protonation to regenerate **Mol 1**.¹² In comparing the different ligands, one can see that the more electron donating pincer, NH₂-POCOP, disfavors acetonitrile coordination the most, while in the CF₃-POCOP pincer, coordination is favorable by 1.2 kcal/mol. This effect will be discussed *vide infra*. **TS 1** is also affected by the electronic effects in the pincer, with the most electron-withdrawing pincer providing the lowest overall barrier at 16.3 kcal/mol, though this is quite close to the barrier for the parent complex (16.9 kcal/mol). Electron donation into the pincer raises the barrier, though likely due to the increased energy required for coordinating MeCN.

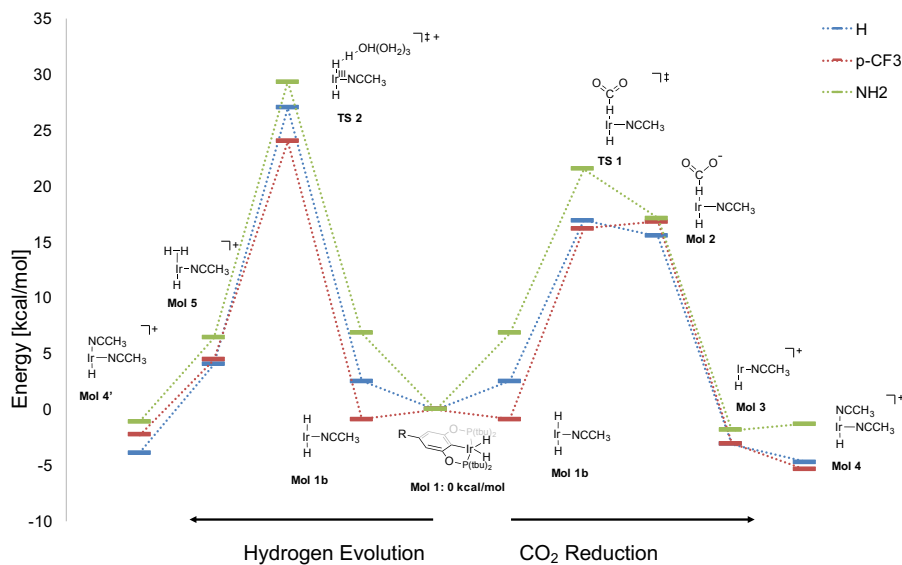


Figure 4.2: Pathways for CO₂ reduction and hydrogen adduct formation are shown for three representative pincer complexes (R-POCOP, X = NH₂, H, CF₃). Free energies in kcal/mol.

Intermediates along the pathway to protonation by water are also shown in Figure 4.2, moving from **Mol 1** in the center to the left. Again, the first step along this pathway is coordination by MeCN. This is followed by protonation by an external four-water cluster (use of which is previously justified^{12,52,53} and is seen in Appendix A.3), represented by **TS 2**. This forms an H₂ adduct, seen in **Mol 5**, which can be released to form the bis-MeCN complex **Mol 4'**. Again, this complex can undergo a two electron reduction and protonation to regenerate **Mol 1**. The lowest barriers again belong to the CF₃-POCOP analogue, at 22.0 kcal/mol. This is 7.3 kcal/mol lower than the NH₂-POCOP analogue. The energy of the H₂ complex **Mol 5** is also affected by the *para* substituent group, with the energy of the electron donating pincer complexes having the highest energy. This again may be attributed to the coordination of MeCN in the axial position.

Both pathways are initiated by the coordination of MeCN in the equatorial position to form **Mol 1b**.¹² The free energy of the formation for all *para* substituted analogues of **Mol 1b** plotted versus Hammett constants (σ) of the substituted functional group is shown in Figure 4.3. Linear correlation between the energy for coordinating MeCN in the equatorial position and the

Hammett constant of the *para* substituted group, shown in Figure 4.3a, implies a strong *trans* influence. The more electron-withdrawing complexes encourage the coordination of MeCN, even driving this energy below zero in the case of CF₃-POCOP, by reducing competition for the orbital shared by the *ipso* carbon in the pincer and MeCN in the equatorial position. This in turn allows for easier donation by the lone pair of MeCN. This *trans* influence has been noted in other pincer complexes with *para* substitutions²⁹ and in iridium complexes with the same functional groups sans pincer directly *trans* to the equatorial position.²⁶ In their work with four and five coordinate complexes with monodentate ligands, Goldman and coworkers showed that little effect is seen unless ligands are directly *trans* to the substituted ligand.²⁶ However, as the pincer complexes are tridentate, the electronic effect of the *para* substitution may be more widely felt by all octahedral positions. This is significant because the relevant H⁻ is in the *cis* position. This is evident in the HOMO diagrams of the CF₃-POCOP and NH₂-POCOP analogues of **Mol 1b**, wherein the π -system of the phenyl ring in the pincer mixes into a combination of the d_{xy} orbital and s orbitals of the hydrides, as shown in Figure 4.3. The NH₂-POCOP analogue shows greater extension into the π -system, even extending into the lone pair of the NH₂ group. The CF₃-POCOP pincer shows greater localization onto the *para* carbon alone.

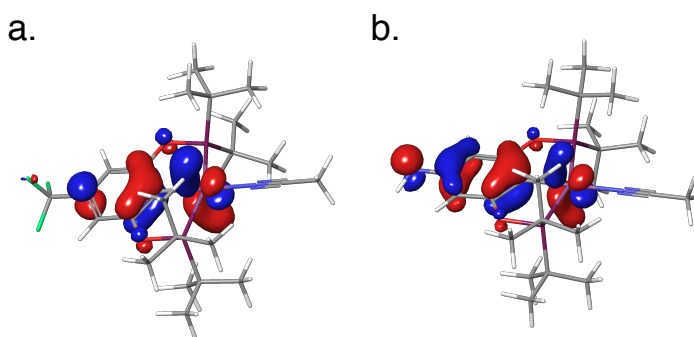


Figure 4.3: HOMO orbitals of a. CF₃-POCOP and b. NH₂-POCOP dihydride. Both analogues show mixing of the π -system of the phenyl ring with the d_{xy} orbitals of the metal.

To separate the geometric effect from the electronic effect of coordinating MeCN, the single point, large basis electronic energy of **Mol 5'** (without the MeCN in the equatorial position, with H₂ *trans* to H⁻) was calculated. This was compared to the electronic energy of **Mol 5**. The results show little change in the energy (< 2 kcal/mol) of the electronic energy for the different substituent groups relative to the energy for coordination, implying that the geometric effect of

moving the H₂ and hydride *trans* to one another is minimal. Additionally, Figure 4.4 also shows the correlation between σ_m Hammett parameters and the free energy of **Mol 1b**. The use of σ_m should remove the effect of π delocalization and resonance and limit the effect to electronegativity effects only. A weaker correlation is seen here, implying that both resonance contributes more strongly and backbonding to the MeCN groups is at play. Backbonding refers to the donation from the d orbitals of the metal back into the p orbitals of the organic ligand, opposite the direction of *sigma* bonding. Backbonding was previously proposed as important in the coordination of acetonitrile⁶ and this work supports that. The impact of these *para* substituted groups is important especially since MeCN coordination is a key step in CO₂RR by (POCOP)Ir.¹²

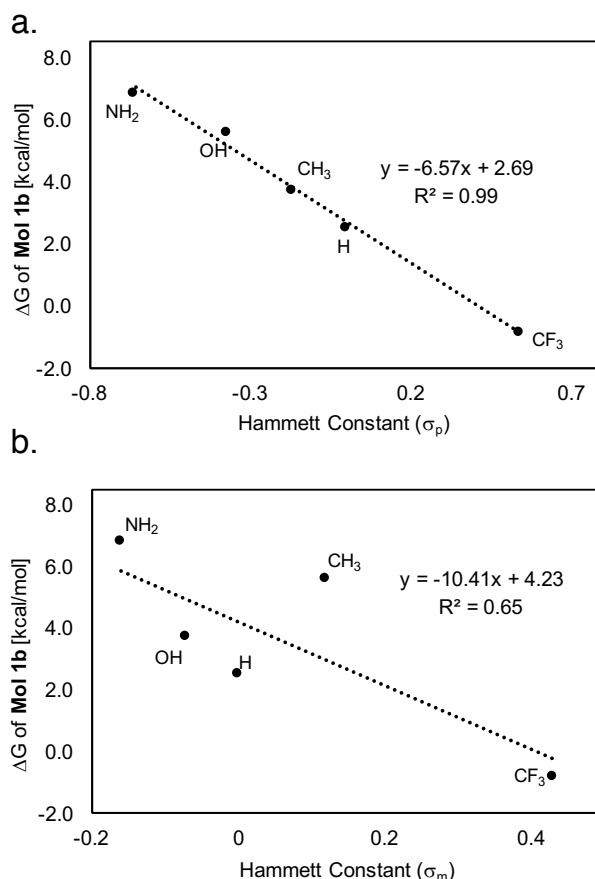


Figure 4.4: Free energy for coordination of acetonitrile versus para (a.) and meta (b.) Hammett constants show that more electron withdrawing group favor acetonitrile coordination.

The substitution of the *para* position in the pincer allows a range of hydricities to be achieved, as shown in Table 4.1. These hydricities allow us to span much of the range of hydricities proposed by Berben et al. that make up the “formate window”. One begins by plotting the Hammett constants versus calculated hydricities. This can be seen in Figure 4.5.

Table 4.1: Hammett constants and calculated hydricities

Functional Group	Hammett Constant (σ_p)	Hammett Constant (σ_m)	Calc'd Hydricity [kcal/mol]
NH ₂	-0.66	-0.16	17.4
OH	-0.37	0.12	17.3
CH ₃	-0.17	-0.07	15.1
H	0.00	0.00	18.6
CF ₃	0.54	0.43	21.0

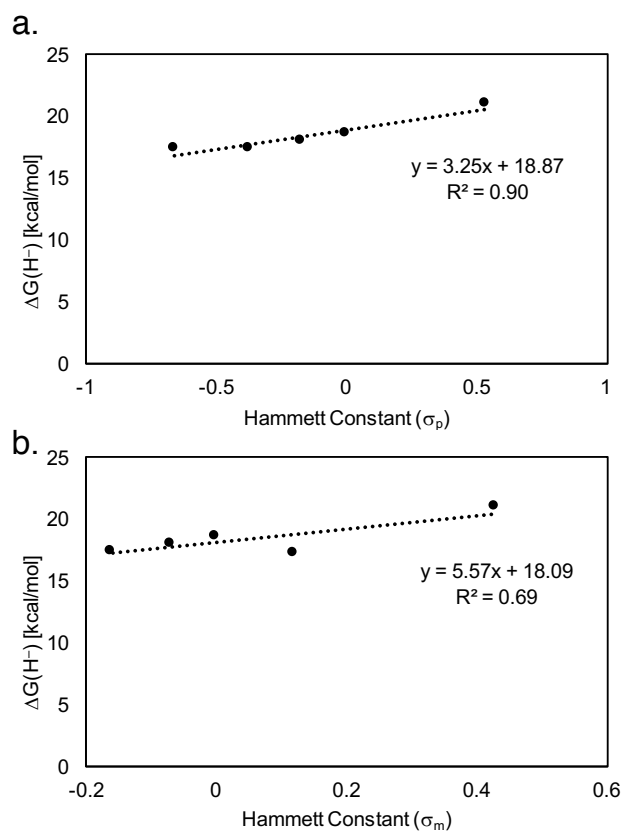


Figure 4.5: Calculated hydricity as a function of *para* and *meta* Hammett constants.

One can see good linear correlation between σ_p and hydricity, with the general trend that electron withdrawing groups lead to less hydridic compounds. Better correlation between σ_p and the calculated hydricities than between σ_m and hydricities imply that this is largely a resonance effect, which can be seen in the previously discussed Figure 4.4.

Hydricities can also be compared to the energies of **TS 1** and **TS 2**. This can be seen in Figure 4.6. It is important to note that all hydricities and barriers are calculated from **Mol 1b** for the sake of consistency. Again, calculated scatter is quite large, particularly in the case of **TS 2**, where no clear trend can be seen. This can be attributed to a number of sources, including the extra degrees of freedom involved in protonation from the water cluster. However, even in the relatively simpler reaction with CO₂ (**TS 1**), little correlation is seen.

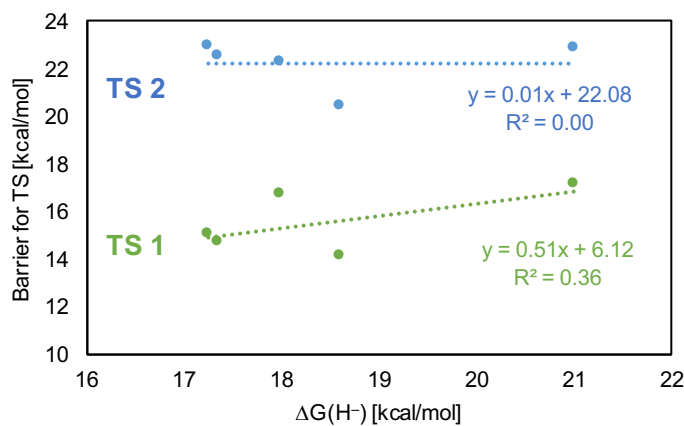


Figure 4.6: Transition states for hydride abstraction by CO₂ (**TS 1**, green) and protonation of hydride (**TS 2**, blue) as a function of hydricity.

While electron withdrawal aids in the initial coordination of MeCN, once MeCN is in the equatorial position, transition state barriers are decreased by electron donating groups. Additional electron density at the metal center may help to break the strong Ir-H bond. From **Mol 1b**, the formation of **Mol 4/4'** is also generally more exergonic for the electron donating groups. Just as solvation of formate by solvent can affect the hydricity,¹² the more exergonic formation of **Mol 4** also provides extra thermodynamic driving force to make electron donating group complexes more hydridic. Increasing hydricity (less thermodynamic driving force) corresponds with higher barriers overall, which would be expected from the Bell-Evans-Polanyi principle.⁵⁴ However, the fact that protonation, which should have a larger driving force, still has

higher barriers overall across the range of hydricities is puzzlingly not in accord with this principle. Despite modifications meant to make this catalyst more reactive to protons, we still see kinetically unfavorable protonation relative to CO₂ reduction and little indication that the trend is changing.

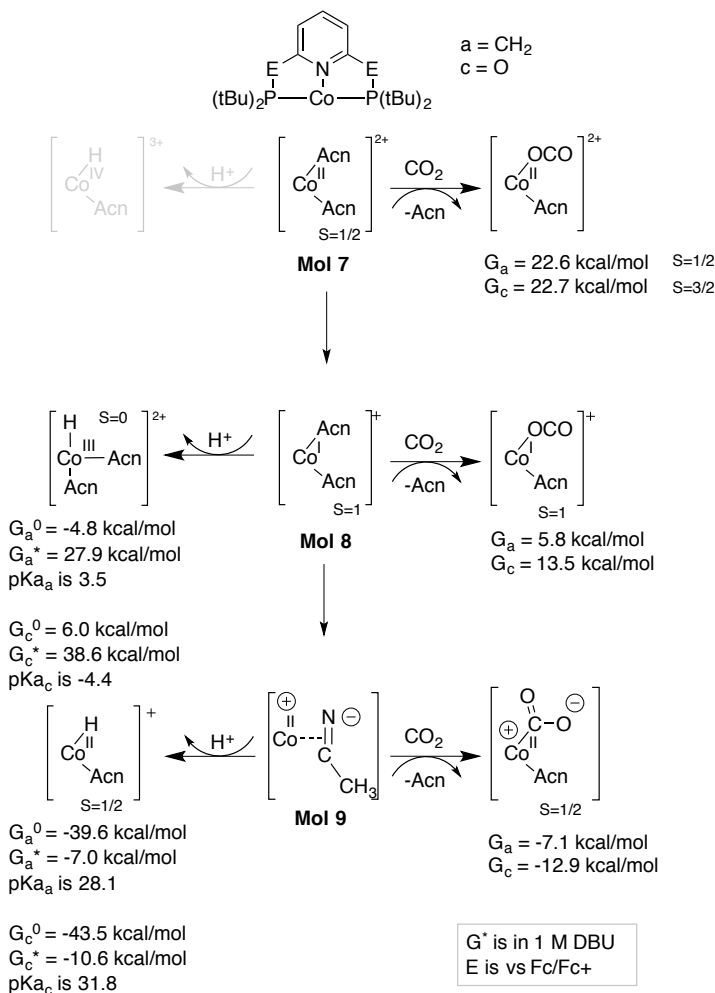
Modification of the *ipso* position

(PENEP)Co catalysts

In work done in conjunction with David Shaffer (now of Brookhaven National Lab) and Prof. Jenny Yang of University of California, Irvine, (PENEP)Co (E = CH₂, O) catalysts were investigated for their use in CO₂RR (seen in Scheme 4.1).⁵⁵ Experimentally, no reaction with the Co^I analogue of these catalysts were seen. However, upon a second reduction event, the (PCNCP)Co analogue did see reaction with CO₂, forming what was spectroelectrochemically identified as a CO bond. This CO adduct of (PCNCP)Co was prepared independently as validation of the carbonyl adduct. Protons are necessary for these compounds to reduce CO₂ to CO and H₂O, which again presents the possibility of competition with HER. Experimentally, the pK_a of (PCNCP)Co was determined to be between 3 and 6 pK_a units, but was difficult to pin down due to the complexes' instability. Therefore, computational methods were employed to gauge the relative intermediate energies involved with a CO₂ versus H⁺ reduction pathway.

Free energies for the reaction of solvento complexes with CO₂ and protons can be seen in Scheme 4.1. For both PCNCP and PONOP ligands, the Co^I and Co^{II} complexes lowest in free energy contain two acetonitrile molecules. The second solvent molecule is weakly bound, by 2.2 kcal/mol relative to liquid MeCN for the PONOP (**Mol 8**) complex. Crystals of related (PNNNP)Co catalysts contain only one bound acetonitrile. The computed association energies are less than the accuracy of DFT free energies, but it is physically reasonable that the weakly bound solvent was liberated by the (drying procedure) used to isolate the crystals. It is thermodynamically unfavorable for the Co^{II} complexes (**Mol 7a** and **Mol 7c**) to react with CO₂, as in both ligands it is uphill by at least 20 kcal/mol to form the CO₂ complex. CO₂ forms a loosely bound complex at the equatorial position through the oxygen. In the PCNCP ligand, the Co-O bond length is calculated to be 2.10 Å and in PONOP the bond length is 2.12 Å.

It is also unfavorable for Co^{I} (**Mol 8a** and **Mol 8c**) to react with CO_2 , and only weakly coordinated complexes form, similar to the Co^{II} case. Protonation of Co^{I} by HDBU (DBU = 1,8-diazabicyclo[5.4.0]undec-7-ene) is also highly endergonic. However, protonation to form $[(\text{PCNCP})\text{Co}^{\text{III}}\text{H}(\text{NCCH}_3)_2]^{+2}$ from **Mol 8a** is accessible with strong acids, giving a calculated pK_a close to the value experimentally measured above. However, **Mol 8c** is calculated to be much less basic, and protonation is not accessible in CH_3CN .



Scheme 4.1: Calculated pK_a values and CO_2 binding energies for the reduction of $[(\text{PCNCP})\text{Co}]$ and $[(\text{POCOP})\text{Co}]$.

At more negative potentials, the Co^{I} cations can be further reduced, as is seen experimentally. While the calculated reduction potentials do not capture the exact values, they do capture the ligand trend. In both PCNCP and PONOP, two kinds of low-energy, formally Co^0 structures

were identified (**Mol 9a** and **9c**). When zero, one or two acetonitrile molecules are coordinated to a neutral (PCNCP)Co moiety through nitrogen, the wavefunction consists of a triplet Co^{I} cation antiferromagnetically coupled to a radical anion ligand with spin distributed around the pyridine ring. The PCNCP ligands can thus become ‘redox active’,^{56,57} but not under conditions for neutral-pH, low-overpotential CO_2 reduction. A few kcal/mol lower in free energy, however, lie neutral (PCNCP)Co(η^1 -C MeCN) complexes incorporating a π -bound solvent molecule. The Mulliken population on bound MeCN ($-0.75e^-$) and C-N and Co-C bond lengths (1.23Å and 1.95Å, respectively) suggest the description of Co^{II} metallacycle. That various isomers lie within 8 kcal/mol of one another underscores how the reduced metal can change coordination at the metal center.

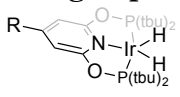
These neutral complexes can react with CO_2 , as it is exergonic by 7.1 kcal/mol in PCNCP and 12.9 kcal/mol in PONOP to do so. This mirrors the experimental findings of this paper, which indicate that reactions with CO_2 occur after the second reduction. With the extra electron density provided by the second reduction, the lone pair from Co is donated into the π^* orbital of the CO_2 , bending the CO_2 adduct. This is similar to the bonding which occurs with the bent MeCN adduct. The competing reaction with protons is also favorable. At pH = 24.3, reacting with protons is exergonic by 7.0 kcal/mol in PCNCP and 10.6 in PONOP.

(PONOP)Ir

While no reaction except at very negative potentials with (PONOP) Co^{I} is seen, it may still be possible for reaction with (PONOP)Ir^{III} dihydride. Previously, Brookhart and coworkers saw evidence of C-H bond cleavage in reactions with benzene.³³ Thus, the reaction of CO_2 with (R-PONOP)Ir was investigated using the same mechanism as previously seen for (POCOP)Ir¹², where X = NH_2 , CH_3 , H, and CF_3 . First, the coordination of MeCN to form **Mol 1b** was investigated, as shown in Table 4.2. While in POCOP the *trans* conformation was preferred¹², this was not the case in all variations of the R-PONOP ligand. Instead, the *cis* conformation was preferred by as much as ~10 kcal/mol in the most electron-donating case of X = NH_2 and ~8 kcal/mol in the most electron-withdrawing case of X = CF_3 . CO_2RR was investigated from the *cis* conformation, but no stable formato complex could be found from either the axial or equatorial hydride, unlike in the POCOP analogues. When the hydricities of these complexes

are compared, it is easy to see why. The *cis* isomer has acetonitrile and pyridine groups *trans* to each hydride. Neither is as good a donor as the hydride or the phenyl ring²⁶ thus the characteristically strong iridium hydride bond cannot be broken. This is reflected in the hydricity, which is 8.6-13.4 kcal/mol too weak to donate to the CO₂/HCOO⁻ couple. These catalysts would not be effective in this manner for CO₂ reduction. It is important to note that another CO₂RR pathway may exist, but that in the case of the dihydride in the presence of acetonitrile, coordination would likely result in the best case, a thermodynamic sink, and in the worst case, hydrogen evolution. In a computational study with a (PCNCP)Ir catalyst, hydrogenation was achievable in both in the case of a trihydride and in the case of a coordinating hydroxyl group in the equatorial position.⁵⁸ This further underlines the importance of a strong *trans* donor in weakening the iridium hydride, as the trihydride is necessary to ensure weakening of the Ir-H bond.

Table 4.2: Free energies for coordination of MeCN to (R-PONOP)Ir complexes.

 R group	ΔG_{trans} [kcal/mol]	ΔG_{cis} [kcal/mol]	Hydricity [kcal/mol]
NH ₂	7.2	-3.3	32.6
CH ₃	5.6	-1.3	32.6
H	5.0	-3.4	34.1
CF ₃	8.2	0.1	37.4

Conclusions

In this study, we investigated the role of modifications on the pincer ligand, both for understanding the relationship between hydricity and kinetics, and general catalytic mechanisms, in (PEXEP)Ir and Co catalysts. Overall, the best candidates for low or accessible barriers involved those with more electron donation to the metal center, as this was important for weakening the Ir-H bond sufficiently for reaction. That being said, electron withdrawal was important in (R-POCOP)Ir catalysts as it allowed for coordination of MeCN. In the case of the dihydride, a strong *trans* influence on the relevant hydride is key in CO₂ reduction from Ir

catalysts, as it further weakens the Ir-H bond, allowing for hydride abstraction. In the case of PENEPC catalysts, neither metal centers are able to complete electrocatalytic CO₂RR without going to very negative potentials, or forming a trihydride, further underlining the importance of electron donation and *trans* effect. Future work in this area involves expanding the data set investigating the relationship between hydricity and barrier height. I propose using several different *para* substituents, particularly in towards the direction of electron donating groups (BH₂, NMe₂). This will expand the range of hydricities achieved, hopefully moving out of the formate window. Additionally, simpler transition states such as the bridging water states in Chapter 2 may also remove some of the noise in the transition state data, giving a cleaner picture of the link between hydricity and barrier height.

References

- (1) Gray, H. B. *Nat. Chem.* **2009**, *1*, 7-7.
- (2) Lewis, N. S.; Nocera, D. G. *Proc. Natl. Acad. Sci. USA* **2006**, *103*, 15729-15735.
- (3) Aresta, M. *Carbon Dioxide Reduction and Uses as a Chemical Feedstock*; Wiley-VCH: Weinheim, Germany, 2006.
- (4) Taheri, A.; Berben, L. A. *Chem. Comm.* **2016**, *52*, 1768-1777.
- (5) Wiedner, E. S.; Chambers, M. B.; Pitman, C. L.; Bullock, R. M.; Miller, A. J. M.; Appel, A. M. *Chem. Rev.* **2016**, *116*, 8655-8692.
- (6) Kang, P.; Chen, Z.; Brookhart, M.; Meyer, T. *Top. Catal.* **2014**, *58*, 30-45.
- (7) Kang, P.; Cheng, C.; Chen, Z.; Schauer, C. K.; Meyer, T. J.; Brookhart, M. *J. Am. Chem. Soc.* **2012**, *134*, 5500-5503.
- (8) Kang, P.; Meyer, T. J.; Brookhart, M. *Chem. Sci.* **2013**, *4*, 3497-3502.
- (9) Kang, P.; Zhang, S.; Meyer, T. J.; Brookhart, M. *Angew. Chem. Int. Ed.* **2014**, *126*, 8853-8857.
- (10) Taheri, A.; Thompson, E. J.; Fettingner, J. C.; Berben, L. A. *ACS Catal.* **2015**, *5*, 7140-7151.
- (11) Taheri, A.; Berben, L. A. *Inorg. Chem.* **2016**, *55*, 378-385.
- (12) Johnson, S. I.; Nielsen, R. J.; Goddard, W. A. *ACS Catal.* **2016**, 6362-6371.
- (13) Connelly, S. J.; Wiedner, E. S.; Appel, A. M. *Dalton Trans.* **2015**, *44*, 5933-5938.
- (14) Cheng, T.-Y.; Brunschwig, B. S.; Bullock, R. M. *J. Am. Chem. Soc.* **1998**, *120*, 13121-13137.
- (15) Jeletic, M. S.; Mock, M. T.; Appel, A. M.; Linehan, J. C. *J. Am. Chem. Soc.* **2013**, *135*, 11533-11536.
- (16) Berning, D. E.; Miedaner, A.; Curtis, C. J.; Noll, B. C.; Rakowski DuBois, M. C.; DuBois, D. L. *Organometallics* **2001**, *20*, 1832-1839.
- (17) Ciancanelli, R.; Noll, B. C.; DuBois, D. L.; DuBois, M. R. *J. Am. Chem. Soc.* **2002**, *124*, 2984-2992.
- (18) Price, A. J.; Ciancanelli, R.; Noll, B. C.; Curtis, C. J.; DuBois, D. L.; DuBois, M. R. *Organometallics* **2002**, *21*, 4833-4839.
- (19) Raebiger, J. W.; Miedaner, A.; Curtis, C. J.; Miller, S. M.; Anderson, O. P.; DuBois, D. L. *J. Am. Chem. Soc.* **2004**, *126*, 5502-5514.
- (20) Creutz, C.; Chou, M. H. *J. Am. Chem. Soc.* **2009**, *131*, 2794-2795.
- (21) Tsay, C.; Livesay, B. N.; Ruelas, S.; Yang, J. Y. *J. Am. Chem. Soc.* **2015**, *137*, 14114-14121.
- (22) Pitman, C. L.; Brereton, K. R.; Miller, A. J. M. *J. Am. Chem. Soc.* **2016**, *138*, 2252-2260.
- (23) Albrecht, M.; van Koten, G. *Angew. Chem. Int. Ed.* **2001**, *40*, 3750-3781.
- (24) Solis, B. H.; Hammes-Schiffer, S. *J. Am. Chem. Soc.* **2011**, *133*, 19036-19039.
- (25) Mondal, B.; Neese, F.; Ye, S. *Inorg. Chem.* **2016**, *55*, 5438-5444.
- (26) Wang, D. Y.; Choliy, Y.; Haibach, M. C.; Hartwig, J. F.; Krogh-Jespersen, K.; Goldman, A. S. *J. Am. Chem. Soc.* **2016**, *138*, 149-163.
- (27) Cheng, M.-J.; Bischof, S. M.; Nielsen, R. J.; Goddard Iii, W. A.; Gunnoe, T. B.; Periana, R. A. *Dalton T.* **2012**, *41*, 3758-3763.
- (28) Sandhya, K. S.; Remya, G. S.; Suresh, C. H. *Inorg. Chem.* **2015**, *54*, 11150-11156.
- (29) Mucha, N. T.; Waterman, R. *Organometallics* **2015**, *34*, 3865-3872.
- (30) Hansch, C.; Leo, A.; Taft, R. W. *Chem. Rev.* **1991**, *91*, 165-195.
- (31) Polukeev, A. V.; Marcos, R.; Ahlquist, M. S. G.; Wendt, O. F. *Organometallics* **2016**, *35*, 2600-2608.
- (32) Hebden, T. J.; St. John, A. J.; Gusev, D. G.; Kaminsky, W.; Goldberg, K. I.; Heinekey, D. M. *Angew. Chem. Int. Ed.* **2011**, *50*, 1873-1876.
- (33) Bernskoetter, W. H.; Hanson, S. K.; Buzak, S. K.; Davis, Z.; White, P. S.; Swartz, R.; Goldberg, K. I.; Brookhart, M. *J. Am. Chem. Soc.* **2009**, *131*, 8603-8613.
- (34) Göttker-Schnetmann, I.; Heinekey, D. M.; Brookhart, M. *J. Am. Chem. Soc.* **2006**, *128*, 17114-17119.
- (35) Shaffer, D. W.; Johnson, S. I.; Rheingold, A. L.; Ziller, J. W.; Goddard, W. A.; Nielsen, R. J.; Yang, J. Y. *Inorg. Chem.* **2014**, *53*, 13031-13041.
- (36) Lee, C. T.; Yang, W. T.; Parr, R. G. *Phys. Rev. B* **1988**, *37*, 785-789.
- (37) Francl, M. M.; Pietro, W. J.; Hehre, W. J.; Binkley, J. S.; Gordon, M. S.; Defrees, D. J.; Pople, J. A. *J. Chem. Phys.* **1982**, *77*, 3654-3665.
- (38) Hehre, W. J.; Ditchfie.R; Pople, J. A. *J. Chem. Phys.* **1972**, *56*, 2257-2261.
- (39) Zhao, Y.; Truhlar, D. G. *Theor. Chem. Acc.* **2008**, *120*, 215-241.
- (40) Martin, J. M. L.; Sundermann, A. *J. Chem. Phys.* **2001**, *114*, 3408-3420.
- (41) Clark, T.; Chandrasekhar, J.; Spitznagel, G. W.; Schleyer, P. V. *J. Comp. Chem.* **1983**, *4*, 294-301.
- (42) Putnam, W. E.; McEachern, D. M. J.; Kilpatrick, J. E. *J. Chem. Phys.* **1965**, *42*, 749-755.

- (43) Kelly, C. P.; Cramer, C. J.; Truhlar, D. G. *J. Phys. Chem. B* **2006**, *110*, 16066-16081.
- (44) Grimme, S.; Antony, J.; Ehrlich, S.; Krieg, H. *J. Chem. Phys.* **2010**, *132*, 154104.
- (45) Dojcansky, J.; Heinrich, J. *Chem. Zvesti* **1974**, *28*, 157-159.
- (46) Chase, M. W. J. *NIST-JANAF Thermochemical Tables, Fourth Edition*, 1998.
- (47) Tissandier, M. D.; Cowen, K. A.; Feng, W. Y.; Gundlach, E.; Cohen, M. H.; Earhart, A. D.; Coe, J. V.; Tuttle, T. R. *J. Phys. Chem. A* **1998**, *102*, 7787-7794.
- (48) Kelly, C. P.; Cramer, C. J.; Truhlar, D. G. *J. Phys. Chem. B* **2006**, *111*, 408-422.
- (49) Kitagawa, Y.; Saito, T.; Ito, M.; Shoji, M.; Koizumi, K.; Yamanaka, S.; Kawakami, T.; Okumura, M.; Yamaguchi, K. *Chem. Phys. Lett.* **2007**, *442*, 445-450.
- (50) Wertz, D. H. *J. Am. Chem. Soc.* **1980**, *102*, 5316-5322.
- (51) Bochevarov, A. D.; Harder, E.; Hughes, T. F.; Greenwood, J. R.; Braden, D. A.; Philipp, D. M.; Rinaldo, D.; Halls, M. D.; Zhang, J.; Friesner, R. A. *Int. J. Quantum Chem.* **2013**, *113*, 2110-2142.
- (52) Creutz, C.; Chou, M. H.; Hou, H.; Muckerman, J. T. *Inorg. Chem.* **2010**, *49*, 9809-9822.
- (53) Huang, Y.; Nielsen, R. J.; Goddard, W. A.; Soriaga, M. P. *J. Am. Chem. Soc.* **2015**, *137*, 6692-6698.
- (54) Evans, M. G.; Polanyi, M. *Trans. Faraday Soc.* **1936**, *32*, 1333-1360.
- (55) Henceforth, for the case where E = CH₂, we will refer to the pincer as PCNCP, with the hydrogens omitted for simplicity.
- (56) Semproni, S. P.; Milsmann, C.; Chirik, P. J. *J. Am. Chem. Soc.* **2014**.
- (57) Khaskin, E.; Diskin-Posner, Y.; Weiner, L.; Leitun, G.; Milstein, D. *Chem. Commun.* **2013**, *49*, 2771-2773.
- (58) Osadchuk, I.; Tamm, T.; Ahlquist, M. S. G. *Organometallics* **2015**, *34*, 4932-4940.